arXiv:1207.2887v1 [cond-mat.str-el] 12 Jul 2012

Spectral properties of Mn doped GaAs: experiment and correlated electronic structure theory

I. Di Marco,[1,*] P. Thunström,[1] M. I. Katsnelson,[2] J. Sadowski,[3]
K. Karlsson,[4] S. Lebègue,[5] J. Kanski,[6] and O. Eriksson[1]

[1] *Department of Physics and Astronomy, Uppsala University, Box 516, SE-75120, Uppsala, Sweden*
[2] *Radboud University Nijmegen, Institute for Molecules and Materials, NL-6525 AJ Nijmegen, The Netherlands*
[3] *MAX-lab, Lund University, SE-22100 Lund, Sweden*
[4] *Department of Life Sciences, Högskolan i Skövde, SE-54128 Skövde, Sweden*
[5] *Laboratoire de Cristallographie, Résonance Magnétique et Modélisations (CRM2, UMR CNRS 7036) Institut Jean Barriol, Nancy Université BP 239, Boulevard des Aiguillettes 54506 Vandoeuvre-lès-Nancy,France*
[6] *Chalmers, Department of Applied Physics, SE-41296 Gothenburg, Sweden*

(Dated: July 13, 2012)

We report an experimental and theoretical study of the valence electron spectrum of the dilute magnetic semiconductor (DMS) material, Mn doped GaAs. The experimental data are obtained through the differences between off- and on-resonance photoemission data for several concentrations of Mn atoms. The theoretical electronic structure is calculated by means of a combination of density-functional theory in the local density approximation and dynamical mean-field theory (LDA+DMFT), using exact diagonalisation as an impurity solver. Theory is found to accurately reproduce measured data, and illustrates the importance of correlation effects in Mn doped GaAs, and that quite likely correlations effects are significant in DMS materials in general. In addition, our results demonstrate the presence of Mn states at the top of the valence band, and we argue that the double-exchange interaction is a significant driving mechanism for the ferromagnetic order in this material.

PACS numbers: 71.20.-b,71.27.+a,75.50.Pp

The field of diluted magnetic semiconductors (DMS) [1, 2] has for the past decade broadened to include several aspects of materials science, e.g. materials synthesis in bulk and thin film form, structural and magnetic characterization, photoelectron spectroscopy for characterization of the electronic structure, and theoretical approaches based on model Hamiltonians or first principles calculations. Several reviews have lately been authored, e.g. in Refs. 3–5, showing the evolution of the field from the first reports on magnetic impurities in semiconductors [6]. A milestone event was the report on carrier-mediated ferromagnetism of Mn-doped InAs and GaAs [1], where the Mn atoms both act as acceptors and magnetic impurities.

In practical applications of spintronics, an ordering temperature above room temperature is needed, and a few systems were predicted [2] to be promising from that point of view, namely Mn-doped ZnO and Mn-doped GaN. Unfortunately, it has proven very difficult to determine their ordering temperatures experimentally, and values ranging from close to 1000K to just above 0 K have been reported. This vast spread of values can possibly be linked to difficulties in synthesizing samples with a homogeneous distribution of substitutional Mn atoms in the host lattice. Mn doped GaAs offers a considerably more robust situation from a synthesis point of view, and substitutional Mn doping at the Ga sites can reach concentrations up to 6-8 %. For the highest concentrations, ordering temperatures (T_C) as high as 170 K [7] to 190 K [8] have been reported and are now generally accepted.

On the theory side, it has been suggested [2] that the ferromagnetic interaction in Mn doped GaAs is described by Vonsovsky-Zener's p-d exchange model [9]. The main assumption of this model is that the Mn-3d electrons are localized and have energies below or close to the bottom of the valence band, which also allows them to induce a hole in the host material. This results in a valence band moment which is coupled anti-ferromagnetically to the impurity 3d moment. The effective exchange interactions between the localized moments is mediated by the conduction carriers of the host, and is argued to be long ranged [2]. Therefore even for dilute doping concentrations, with Mn atoms distributed far apart, a significant ferromagnetic coupling between transition metal moments was suggested to be possible [2].

However, recent experimental studies of Mn doped GaAs [10] point to that the Fermi level is situated essentially in the band gap, not in the valence band, and this casts doubts on the applicability of the p-d exchange model. Furthermore, the picture of long-ranged interactions has also been challenged by calculations based on first principles theory. In this case a much more short ranged interaction is observed in general, with magnetic percolation as a key ingredient, and a decent agreement is found between calculated and observed ordering temperature [11, 12]. In addition, the works based on first principles theory suggest a different location of the Mn-3d states, lying at the top of the valence band, and forming a strongly hybridized state [4]. This has implications for the mechanism of magnetic ordering, and in Refs. 4 and 13 it was suggested that the electronic structure of Mn doped GaAs has a significant contribution from the double exchange mechanism, and that the range of the interaction was short. Most of these calculations are based on a mean-field like description of the electronic structure via density functional theory (DFT) in the local density approximation (LDA) or the generalized gradient approximation (GGA). The main criticism to this theory is that a mean-field like description may not be sufficiently accurate for describing the Mn-3d states, and that correlation effects due to the strong Coulomb interaction must be considered [5].

The discussion above indicates that a thorough analysis of the electronic structure of Mn doped GaAs is highly needed, combining experimental data with accurate theory, to ease the interpretation. Recent studies regarding the coupling of the electronic structure to the nature of the magnetic interactions further highlight this need [14]. The purpose of this letter is indeed to provide such an analysis, and we present here the spectral properties of Mn doped GaAs as given by differences between off- and on-resonance photoemission data for 0.1, 1 and 6 % Mn doping. The experimental results are compared with electronic structure calculations based on a combination of density-functional theory in local density approximation and dynamical mean-field theory (LDA+DMFT) [15, 16].

The photoemission data were obtained at the Swedish synchrotron radiation facility MAX-lab using the surface end station of the I511 undulator beamline [17]. The samples were prepared in a local molecular beam epitaxy (MBE) system, and were transferred to the photoemission station in a portable UHV chamber without being exposed to atmosphere. The Mn concentrations were determined during growth by means of reflection high-energy electron diffraction (RHEED) oscillations, as described earlier [18]. All spectra presented here were obtained from as-grown samples, i.e. samples not subjected to post-growth annealing.

Valence band spectra were recorded at two photon energies, one on the $2p_{3/2}$ absorption peak (A in the inset of Fig. 1), the other 2 eV below the peak (B in the inset of Fig. 1), and the Mn-3d resonant emission was obtained from the difference between the two spectra. In a previous study [19] corresponding structures were extracted by combining spectra from (Ga,Mn)As and clean GaAs obtained at the same excitation energy. The main advantage of the procedure adopted here is that it avoids artifacts that inevitably arise due to different surface states on different surfaces. In the extraction of difference spectra it is of course important, particularly in the most dilute cases, that the spectra are properly normalized and aligned in energy. This was accomplished by including the Ga-3d peak in the recorded energy range. By means of this peak the spectra could be aligned with a precision of 1 meV, and the normalization was checked via the absence of any systematic structures in the energy region of Ga-3d emission. For the most dilute cases it turned out that thermal effects, mainly associated with gradual monochromator heating had to be taken into account. To minimize these effects, the recording time for each pair of spectra was reduced to about 2 minutes. To achieve reasonable statistics, a number of difference spectra (typically 50-100) were added after proper alignment.

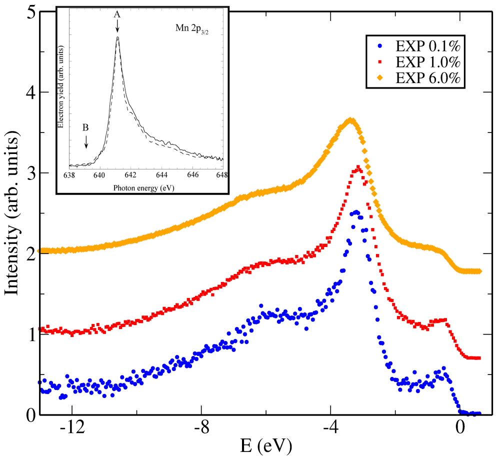

FIG. 1. (color online) Resonant photoemission spectra of Mn-3d states in Mn doped GaAs at several concentrations. In the inset the Mn $2p_{3/2}$ XAS spectra with 0.3 % and 6 % Mn (dashed and solid lines, respectively) are shown. "A" and "B" indicate the two photon energies used for extracting the resonant photoemission spectra.

The theoretical spectra have been calculated by means of a LDA+DMFT code [20] based on a full-potential linear-muffin tin orbital method (FP-LMTO) [21], which is particularly suitable for large supercell geometries. The Mn doped GaAs was modeled with a supercell $Ga_{26}MnAs_{27}$, corresponding to a Mn concentration of 3.75%. The experimental lattice constant $a = 10.681$ a.u. was used, and the Brillouin zone was sampled with a mesh of 256 **k**-points. The LDA+DMFT scheme was applied to explicitly treat the local Coulomb interaction between the localized Mn-3d electrons. The 4-index rotationally-invariant Coulomb interaction matrix was generated from the Slater parameters F^0, F^2 and F^4. The choice of the average Coulomb repulsion F^0, which corresponds to the Hubbard U, is rather problematic, since no calculations based on constrained LDA or RPA methods are found in literature. Therefore we have considered values between 4 eV and 7 eV, which are the accepted strengths of the Coulomb repulsion for bulk metallic γ-Mn [22] and MnO [23]. The main results of the paper are presented for the intermediate value U = 6 eV, while the effects due to the variation of the Hubbard parameter are discussed at the end. F^2 and F^4 are easier to evaluate,

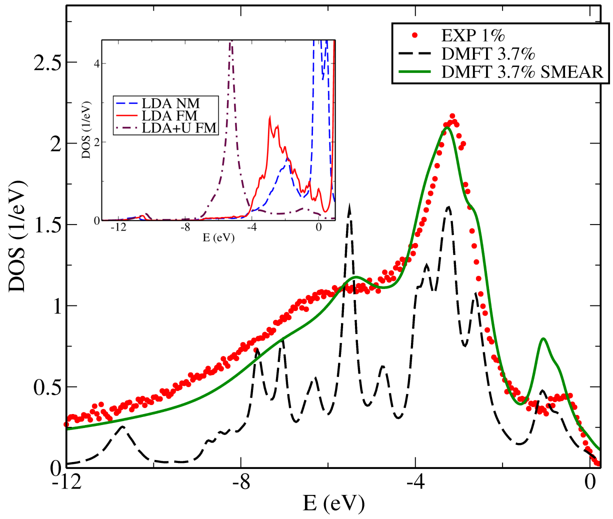

FIG. 2. (color online) Resonant photoemission spectrum of Mn-3d states in Mn doped GaAs at 1% concentration compared to the Mn-3d projected density of states from LDA+DMFT, with and without Lorentzian smearing. The Fermi level is at zero energy, and no artificial shifts have been applied between theoretical and experimental curves. In the inset the ferromagnetic (FM) and non-magnetic (NM) LSDA results are shown, together with the LDA+U results.

and therefore were calculated directly from the electronic density, as for MnO in Ref. 24. These values correspond to the average Hund's exchange parameter J $\simeq$ 1 eV.

The effective impurity problem arising in LDA+DMFT has been solved through exact diagonalisation (ED) method, as described in Ref. 24. The fermionic bath interacting with the atomic impurity has been approximated by means of 22 auxiliary bath sites: 18 bath sites were coupled to the strongly hybridizing Mn t_{2g} states, while only 4 bath sites were coupled to the weakly hybridizing Mn e_g states. Notice that the full diagonalisation of a model containing a total of 32 states (22 bath sites plus 10 atomic orbitals) is already extremely demanding from the computational point of view, due to the fact that full temperature dependence is considered [24]. Finally we should mention that all the calculations have been made for the paramagnetic phase at T = 400 K and using 1200 fermionic Matsubara frequencies. The double counting problem has been considered in the fully localized limit (FLL) [15].

In Fig. 1 the experimental data for the Mn-3d one-particle excitation spectrum are reported for samples with a Mn concentration of 0.1%, 1%, and 6%. The curves were extracted by taking differences between off- and on-resonance photon energies for the Mn-3d cross section. In Fig. 2 the experimental spectrum for the sample with 1% Mn concentration is directly compared with the LDA+DMFT projected density of states (PDOS) of the Mn-3d orbitals, for 3.7% Mn concentration. For such concentrations of Mn, the direct wave-function overlap between different Mn atoms is vanishingly small, and it is expected that the spectral properties are rather insensitive to smaller modifications of the Mn concentration (as Fig. 1 also shows). Hence it is possible to compare experiment for a Mn concentration of 1% with theory for a 3.7% Mn concentration. Note that we in Fig. 2 show theoretical data, unbroadened and directly as obtained from the DMFT calculation, as well as theory which has been broadened due to life-time effects. The broadening considered was obtained from Fermi-Liquid theory, in which the life-time broadening grows quadratically with the binding energy. As is clear from Fig. 2, both experiment and theory position the Mn-3d states primarily in the valence band of the GaAs host, with an important feature that the Mn-3d states extend over a broad range of energies. The Fermi level is pinned by a Mn-3d band, which is situated at the top of the valence band of the GaAs host. This feature is in good agreement with the recent experimental results of Ref. 10, and has important consequences on the nature of the magnetic interactions, as discussed below. The experimental spectrum has a main peak at $\sim$ 3.2 eV biding energy, an observation that is captured by theory. Furthermore, the observed broad shoulder, which is located between 4 and 8 eV binding energy, is also well described in the LDA+DMFT excitation spectrum. Overall, the agreement between theory and experiment must be judged as being good. Only in the closest region to the Fermi level can one notice some discrepancies between theory and experiment, where the small peak at $\sim$ 1 eV binding energy has a slightly too large intensity in the calculations, when compared to observations.

In the inset of Fig. 2 the Mn-3d PDOS for non-magnetic and magnetic LSDA are reported, and we note that the agreement with the experimental data is less satisfactory. The entire spectral weight is in this case concentrated relatively close to the Fermi level, and while the position of the main peak is almost correct, the large shoulder at higher binding energy is totally absent. If static correlations are added [25], as for the LDA+U simulations shown in the same inset, the agreement with the experiment does not improve much: from the basically correct LDA position the main peak is moved to lower energies, depending on the value of U, but it is not possible to describe the broad distribution of spectral weight from the Fermi level down to -8 eV, and in particular the observed spectral features in at binding energies between 4 and 8 eV. The LDA and LDA+U deficiencies are related to the fact that they are basically single Slater determinant theories, and only the inclusion of dynamical many-body effects is able to capture the satellite-like features of the Mn-3d excitation spectrum. These problematic aspects of correlated electronic structures are closely related to recent findings [24, 26] for the charge-transfer insulator NiO, where experimental data show a broad distribution of Ni-3d spectral weight not

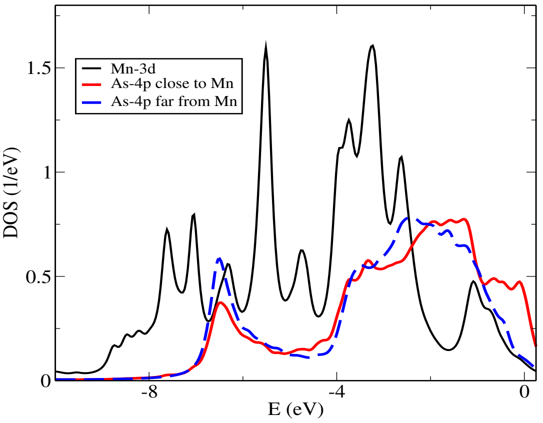

FIG. 3. (color online) LDA+DMFT PDOS of the Mn-3d electrons and As-4p electrons, close and far from the Mn ions. The Fermi level is at zero energy.

describable within one-particle approximations, but well reproduced by LDA+DMFT.

In Fig. 3 we report the calculated PDOS for the As-4p states, which are the main contributors to the valence band, both for an As atom far away from the impurity Mn atom and for an As atom close to the Mn atom. As seen by inspection of the states projected on the As atom far from the Mn impurity, the Fermi level is located above the band edge of the valence band. The p-states of the As atom close to the Mn atom show some hybridization with the Mn-3d states. These results rule out the presence of a hole in the valence band that extends over a long range, it is in fact primarily located on As atoms in the nearest vicinity of the Mn atom.

Our results draw a physical picture of an impurity band formation within the band gap, composed of As 4p states and Mn 3d states, as also suggested by recent experimental results [10]. Previous DMFT studies on model systems [27] are also consistent with this scenario, if the parametrized exchange interactions between Mn spins and carriers spins are strong enough. Overall our theoretical and experimental electronic structure rules out a pure pd-exchange mechanism in Mn doped GaAs, and points to the fact that a significant contribution from the double-exchange mechanism must take place [12], where conduction and magnetic electrons belong to the same band. In this situation (described by a Hubbard-like model) the exchange interactions can be of essentially non-Heisenberg character [16, 28].

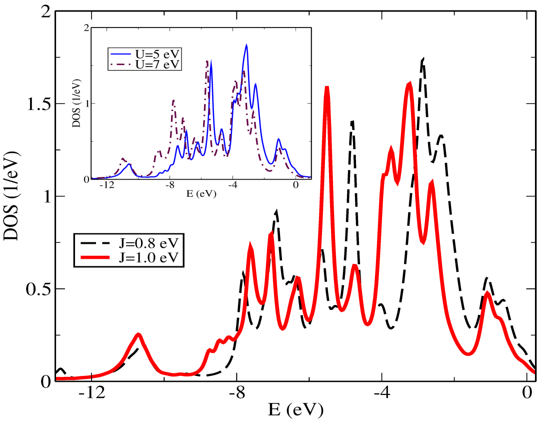

FIG. 4. (color online) LDA+DMFT PDOS of the Mn-3d electrons for different values of the exchange parameter J. In the inset the same information is shown for different values of U. The Fermi level is at zero energy.

We also want to stress that the precise choice of the Hubbard parameter U within a reasonable range of values, does not lead to qualitative differences in the LDA+DMFT spectral properties. In the inset of Fig. 4 the Mn-3d PDOS for U=5 eV and U=7 eV are reported. Even for these important changes of U, the main features of the two curves remain similar to what observed in Fig. 2, and only a small redistribution of spectral weight at higher binding energies can be observed. In Fig. 4 the LDA+DMFT Mn-3d PDOS for U=6 eV and J=0.8 eV [29] is compared with our calculated data for J=1 eV. The general features of the spectrum are the same, but the two main peaks are shifted towards the Fermi level in the simulation with lower J. From these results we can see that a change of the parameters in the calculation only worsens the agreement with experimental data and does not change the physical picture outlined in this letter.

In conclusions we have studied the spectral properties of Mn doped GaAs, in a joint experimental and theoretical effort, based on LDA+DMFT, using exact diagonalisation as an impurity solver. Theory is found to accurately reproduce measured data, which points to the importance of correlation effects in Mn doped GaAs, and that quite likely correlation effects are significant in DMS materials in general. In addition, our results demonstrate the presence of Mn states at the top of the valence band, which is consistent with recent experimental observations [10]. This rules out a pure pd-exchange mechanism, and points to that the double-exchange interaction is a significant driving mechanism for the ferromagnetic order in this material.

ACKNOWLEDGMENT

Financial support from the Swedish Research Council (VR) and Energimyndigheten (STEM), is acknowledged. Calculations have been performed at the Swedish national computer centers UPPMAX, PDC, HPC2N and NSC. O.E. is also grateful to the European Research Council (grant 247062 - ASD) and the Knut and Alice Wallenberg Foundation, for financial support.

---

[*] igor.dimarco@physics.uu.se

[1] H. Ohno, Science **281**, 951 (1998).

[2] T. Dietl, H. Ohno, F. Matsukura, J. Cibert, and D. Ferrand, Science **287**, 1019 (2000).

[3] A. Zunger, "Solid state physics," (Academic Press, 1986); T. Jungwirth, J. Sinova, J. Mašek, J. Kučera, and A. H. MacDonald, Rev. Mod. Phys. **78**, 809 (2006); F. Pulizzi, Nature Materials (2008), 10.1038/nphys872, doi:10.1038/nphys872.

[4] K. Sato, L. Bergqvist, J. Kudrnovský, P. H. Dederichs, O. Eriksson, I. Turek, B. Sanyal, G. Bouzerar, H. Katayama-Yoshida, V. A. Dinh, T. Fukushima, H. Kizaki, and R. Zeller, Rev. Mod. Phys. **82**, 1633 (2010).

[5] T. Dietl, Nature Materials **9**, 965 (2010).

[6] R. W. Cochrane, M. Plischke, and J. O. Ström-Olsen, Phys. Rev. B **9**, 3013 (1974); T. Story, R. R. Gałązka, R. B. Frankel, and P. A. Wolff, Phys. Rev. Lett. **56**, 777 (1986).

[7] K. W. Edmonds, K. Y. Wang, R. P. Campion, A. C. Neumann, C. T. Foxon, B. L. Gallagher, and P. C. Main, Applied Physics Letters **81**, 3010 (2002).

[8] L. Chen, S. Yan, P. F. Xu, J. Lu, W. Z. Wang, J. J. Deng, X. Qian, Y. Ji, and J. H. Zhao, Applied Physics Letters **95**, 182505 (2009).

[9] S. V. Vonsovsky, Zh. Eksp. Teor. Fiz. **16**, 981 (1946); C. Zener, Phys. Rev. **81**, 440 (1951).

[10] S. Ohya, I. Muneta, P. N. Hai, and M. Tanaka, Phys. Rev. Lett. **104**, 167204 (2010).

[11] L. Bergqvist, O. Eriksson, J. Kudrnovský, V. Drchal, P. Korzhavyi, and I. Turek, Phys. Rev. Lett. **93**, 137202 (2004).

[12] K. Sato, W. Schweika, P. H. Dederichs, and H. Katayama-Yoshida, Phys. Rev. B **70**, 201202 (2004).

[13] S. Sanvito, P. Ordejón, and N. A. Hill, Phys. Rev. B **63**, 165206 (2001).

[14] M. Dobrowolska, K. Tivakornsasithorn, X. Liu, J. K. Furdyna, M. Berciu, K. M. Yu, and W. Walukiewicz, Nature Materials **11**, 444 (2012); N. Samarth, Nature Materials **11**, 360 (2012).

[15] G. Kotliar, S. Savrasov, K. Haule, V. Oudovenko, O. Parcollet, and C. Marianetti, Rev. Mod. Phys. **78**, 865 (2006); K. Held, Advances in Physics **56**, 829 (2007).

[16] M. I. Katsnelson, V. Y. Irkhin, L. Chioncel, A. I. Lichtenstein, and R. A. de Groot, Rev. Mod. Phys. **80**, 315 (2008).

[17] R. Denecke, P. Väterlein, M. Bässler, N. Wassdahl, S. Butorin, A. Nilsson, J.-E. Rubensson, J. Nordgren, N. Mårtensson, and R. Nyholm, Journal of Electron Spectroscopy and Related Phenomena **101103**, 971 (1999).

[18] J. Sadowski, J. Z. Domagala, J. Bak-Misiuk, S. Kolesnik, M. Sawicki, K. Swiatek, J. Kanski, L. Ilver, and V. Strom, J. Vac. Sci. Technol. B **18**, 1697 (2000).

[19] O. Rader, C. Pampuch, A. M. Shikin, W. Gudat, J. Okabayashi, T. Mizokawa, A. Fujimori, T. Hayashi, M. Tanaka, A. Tanaka, and A. Kimura, Phys. Rev. B **69**, 075202 (2004).

[20] A. Grechnev, I. Di Marco, M. I. Katsnelson, A. I. Lichtenstein, J. Wills, and O. Eriksson, Phys. Rev. B **76**, 035107 (2007); I. Di Marco, J. Minár, S. Chadov, M. I. Katsnelson, H. Ebert, and A. I. Lichtenstein, Phys. Rev. B **79**, 115111 (2009); O. Grånäs, I. Di Marco, P. Thunström, L. Nordström, O. Eriksson, T. Björkman, and J. Wills, Computational Materials Science **55**, 295 (2012).

[21] J. M. Wills, M. Alouani, P. Andersson, A. Delin, O. Eriksson, and O. Grechnyev, *Full-Potential Electronic Structure Method*, edited by H. Dreysse, Electronic Structure and Physical Properties of Solids: Springer Series in Solid-State Sciences (Springer-Verlag, Berlin, 2010).

[22] S. Biermann, A. Dallmeyer, C. Carbone, W. Eberhardt, C. Pampuch, O. Rader, M. I. Katsnelson, and A. I. Lichtenstein, Pis'ma ZhETF **80**, 714 (2004), [JETP Letters **80**, 614 (2004)]; I. Di Marco, J. Minár, J. Braun, M. I. Katsnelson, A. Grechnev, H. Ebert, A. I. Lichtenstein, and O. Eriksson, Eur. Phys. J. B **72**, 473 (2009).

[23] J. Kuneš, A. V. Lukoyanov, V. I. Anisimov, R. T. Scalettar, and W. E. Pickett, Nat. Mater. **7**, 198 (2008).

[24] P. Thunström, I. Di Marco, and O. Eriksson, "Electronic entanglement in late transition metal oxides," ArXiv:1202.3975.

[25] J. Park, S. Kwon, and B. Min, Physica B: Condensed Matter **281–282**, 703 (2000); B. Sanyal, O. Bengone, and S. Mirbt, Phys. Rev. B **68**, 205210 (2003); L. M. Sandratskii, P. Bruno, and J. Kudrnovský, Phys. Rev. B **69**, 195203 (2004); A. B. Shick, J. Kudrnovský, and V. Drchal, Phys. Rev. B **69**, 125207 (2004).

[26] J. Kuneš, V. I. Anisimov, A. V. Lukoyanov, and D. Vollhardt, Phys. Rev. B **75**, 165115 (2007); J. Kuneš, V. I. Anisimov, S. L. Skornyakov, A. V. Lukoyanov, and D. Vollhardt, Phys. Rev. Lett. **99**, 156404 (2007).

[27] L. Craco, M. S. Laad, and E. Müller-Hartmann, Phys. Rev. B **68**, 233310 (2003); M. A. Majidi, J. Moreno, M. Jarrell, R. S. Fishman, and K. Aryanpour, Phys. Rev. B **74**, 115205 (2006); F. Popescu, Y. Yildirim, G. Alvarez, A. Moreo, and E. Dagotto, Phys. Rev. B **73**, 075206 (2006); F. Popescu, C. Şen, E. Dagotto, and A. Moreo, Phys. Rev. B **76**, 085206 (2007).

[28] M. Auslender and M. Katsnelson, Solid State Communications **44**, 387 (1982), Teor. Mat. Fiz. 51, 436 (1982).

[29] Here F^2 and F^4 have been obtained by means of fixed atomic ratios [15].